Kinematically Complete Study of Dissociative Ionization of D_2 by Ion Impact

G. Laurent,[1,2] J. Fernández,[2] S. Legendre,[1] M. Tarisien,[1] L. Adoui,[1] A. Cassimi,[1] X. Fléchard,[3] F. Frémont,[1] B. Gervais,[1] E. Giglio,[1] J. P. Grandin,[1] and F. Martín[2]

[1]*Centre Interdisciplinaire de Recherche Ions Lasers (CIRIL)—CEA-CNRS-ENSICaen, rue Claude Bloch, BP 5133, F-14070 Caen cedex 5, France*

[2]*Departamento de Química C-9, Universidad Autónoma de Madrid, 28049 Madrid, Spain*

[3]*LPC-Caen, 6 Bd du Maréchal Juin, F-14050 Caen cedex, France*

(Received 30 November 2005; published 1 May 2006)

We present a kinematically complete study of dissociative ionization of D_2 by 13.6 MeV/u S^{15+} ions. The experiment allows us to unravel the competing mechanisms, namely, direct single ionization, autoionization of doubly excited states, ionization excitation, and double ionization, and to analyze the corresponding electron angular distribution from fixed-in-space molecules. The conclusions are supported by theoretical calculations in which the correlated motion of all electrons and nuclei and the interferences between them are described from first principles.

DOI: 10.1103/PhysRevLett.96.173201 PACS numbers: 34.50.Gb

Ionization of the simplest H_2 molecule by the impact of photons [1–7], electrons [8–11], and ions [12–18] has been the subject of extensive experimental and theoretical investigations for almost three decades. With the advent of kinematically complete collision experiments, in which the full momentum vector of all charged particles is determined, it is now possible to investigate these processes with unprecedented detail and precision. So far a few examples have been reported in the literature for photoionization [19–23] and electron impact ionization [24].

In contrast with photoionization, in which a well-defined amount of energy is absorbed by the target (the photon energy), the energy absorbed by H_2 in a collision with a fast charged projectile follows a distribution with practically no upper limit. Thus all processes capable of ionizing the molecule are energetically allowed and can, in principle, occur simultaneously. It also means that ionization can involve one or all electrons of the molecule. In the case of ion impact, the only existing electron-ion coincidence experiment has been reported by Dimopoulou *et al.* [25]. In this work both nondissociative and dissociative ionization of H_2 were investigated in the range of very low ion kinetic energy (<0.04 eV). However, it has been shown in previous experiments [26] that major dissociating processes lead to proton energies as large as 12 eV. In the present Letter we present a kinematically complete experimental study of the collision between 13.6 MeV/u S^{15+} ions and D_2 molecules. We detect in coincidence all ejected ions and electrons in the whole energy range accessible in the collision. The experiment allows us to unravel the competing mechanisms leading to dissociative ionization of D_2. The measurements are supported by theoretical calculations in which the motion of all electrons and nuclei as well as correlations and interferences between them are described from first principles.

It is known that the dominant ionization process is emission of a single electron that leaves the residual D_2^+ molecular ion in its ground $^2\Sigma_g^+$ electronic state [16]. Most of the D_2^+ ions remain in a bound vibrational level (around $v = 2$), while only a few undergo dissociative single ionization (DSI). Two-electron processes also contribute to ionization: ionization excitation (IE), double ionization (DI), and double excitation followed by autoionization (AI). In DI, both electrons are emitted into the continuum through a direct nonresonant ionization process, leading to a D_2^{2+} molecular ion that dissociates through Coulomb explosion. In IE, only one electron is emitted into the continuum, while D_2^+ is formed in an excited electronic state that dissociates. DSI, IE, and DI are direct ionization processes. In contrast, AI is a resonant process that results from the decay of a doubly excited state (DES) into the ionization continuum. The corresponding D_2^+ ion can remain in either the ground or an excited electronic state [4]. Since the DES potential energy curves are repulsive, dissociation into two neutral D atoms also competes with AI. There is a series of DESs, Q_n, associated with each ionization threshold, n (i.e., associated with each electronic state of D_2^+). Each series contains an infinite number of DESs, and there is an infinite number of such series. Previous photoionization experiments have shown that the DESs play a crucial role in dissociative ionization of D_2 [3] and the same is expected in the present case.

It is then clear that the number of open channels leading to dissociative ionization is so large that only an experimental approach that images all charged particles in coincidence can disentangle the different mechanisms. Such an experiment has been performed at GANIL in Caen. A 13.6 MeV/u S^{15+} projectile beam intersected a D_2 supersonic molecular gas jet. The D^+ fragments up to 12 eV are collected by a static electric field (30 V/cm) with 4π solid angle acceptance and directed onto a 80 mm diameter position sensitive channel-plate detector. In addition, a magnetic field (18 G) confines the electrons on helical trajectories, ensuring a 4π solid angle coverage for kinetic ener-

gies up to 55 eV. From both the time of flight and coordinates of impact position of each particle detected, the complete momentum vector of the electrons and fragment ions were then reconstructed and the energy deduced ($\Delta E/E =$ 15% and 5% for electrons and ions, respectively).

The complete ion-electron energy correlation diagram is shown in Fig. 1(a). The result has been integrated over the emission angles of both electrons and ions. As expected, the energy sharing between electrons and nuclei is much more complex than in photoionization processes in which an almost linear dependence between electron and ion kinetic energies is observed [21]. The latter behavior is the consequence of energy conservation, $E_{e^-} = -2E_{D^+} + E_T - E_\infty$, where E_{e^-} is the electron kinetic energies, E_{D^+} is the D^+ kinetic energies, E_T is the total energy transferred to the molecule, and E_∞ is the dissociation energy limit. We can see a similar behavior for D^+ energies between 1 and 4 eV. This is because, in the case of resonant dissociative ionization through a DES, E_T is more or less fixed and so is the difference $E_T - E_\infty$.

The electron and D^+ energy distributions are shown in Figs. 1(a) and 2(a), respectively. In the latter case, an analysis of the coincidence measurements allows us to extract the contribution of each dissociative process [Fig. 2(a)]. The total D^+ distribution agrees qualitatively with that previously measured by Edwards *et al.* [26] using a different projectile and a different impact velocity. The D^+ energy distribution associated with the AI process is determined by integrating the Auger peaks observed in the electron energy distribution for a specific D^+ energy range. In doing so, one assumes that resonant and nonresonant processes sum up incoherently, which is not strictly true [4] but is a reasonable approximation in the present case since DSI and AI appear in separate regions of the e^--D^+ diagram (except for very low D^+ energies). Subtraction of this AI contribution from the total D^+ distribution allows us to separate the DSI contribution (localized on the low energy side) from the DI + IE one (localized on the high energy side); see Fig. 2(a). The shape of the DI distribution is obtained from coincident detection of two D^+ fragments. We have found that this shape is very close to the corresponding Franck-Condon (FC) factor. The relative contribution of this process has been deduced from the known DI/IE cross-section ratio [16], which is ~20% for a large variety of projectiles with charge q and velocity v satisfying the condition $0.1 < q/v < 1.5$. In the present experiment, $q/v = 0.7$. All contributions are shown in Fig. 2(a).

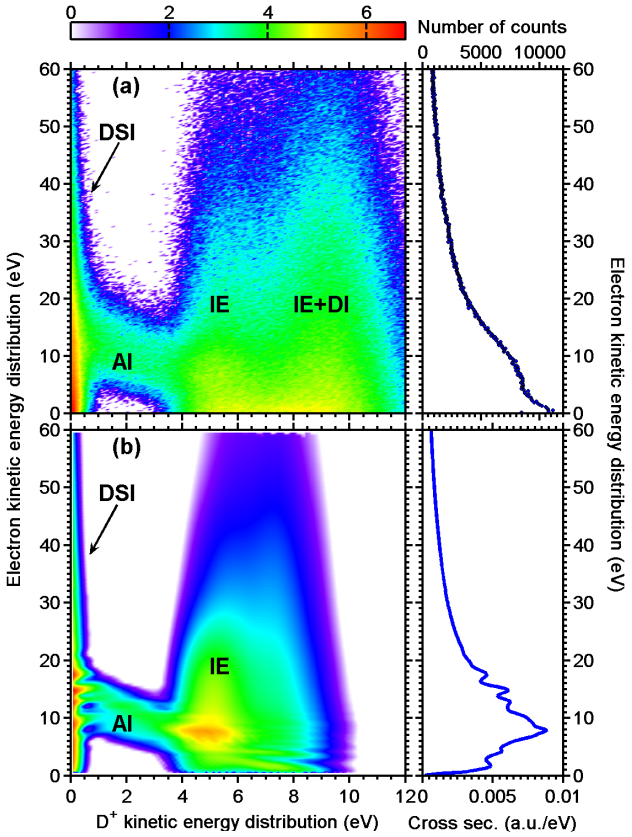

FIG. 1 (color online). Electron and D^+ kinetic energy correlation diagram resulting from a 13.6 MeV/u S^{15+}-D_2 collision. (a) Experimental results. IE, ionization excitation; AI, autoionization; DI, double ionization; DSI, direct single ionization. (b) Theoretical results. The right panels show integration over D^+ energy.

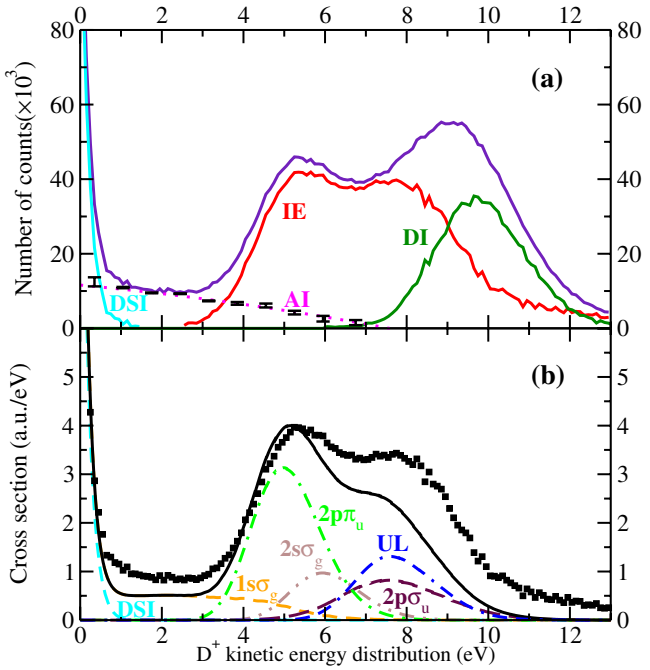

FIG. 2 (color online). D^+ kinetic energy distribution for the 13.6 MeV/u S^{15+}-D_2 collision. (a) Experimental results (error bars are shown for illustration). (b) Theoretical results for DSI + AI + IE (solid line) compared to experimental results (squares). Contributions from the $1s\sigma_g$, $2p\sigma_u$, $2p\pi_u$, and $2s\sigma_g$ ionization thresholds are shown separately. Contributions from upper ionization thresholds (UL) are shown together.

Relative cross sections for each process have been obtained by integrating the D^+ energy distributions. We have found that dissociative ionization is only $6.2 \pm 1.2\%$ of the total ionization cross section. Relative contributions to dissociative ionization from the different processes are as follows: DSI, $7.3 \pm 1.8\%$; AI, $13.0 \pm 2.7\%$; IE, $64.6 \pm 7.5\%$; DI, $15.1 \pm 4.4\%$. The contribution of DSI to the total nondissociative single ionization is 0.48%, close to the value 0.485% determined by Ben-Itzhak *et al.* [27].

To better understand the origin of the structures observed in the experiment, we have evaluated angle integrated cross sections, differential in both electron and D^+ energies, in the framework of the first Born and dipole approximations using Eq. (1) of Ref. [11]. The initial and final D_2 states have been evaluated in the adiabatic approximation using the theory of [28] [see also Eqs. (42) and (60) of Ref. [29]]. Briefly, the final state results from a close-coupling calculation that includes contributions from the ten lowest ionization thresholds of D_2, the Q_1, Q_2, Q_3, and Q_4 doubly excited states [30–32], as well as the corresponding vibrational and dissociative states. Therefore, it is not simply given by the product of an electronic and a nuclear wave function, but by a more complex form that accounts for interferences among the various electronic and nuclear channels. DSI has been obtained by excluding all Q states and all IE channels from the close-coupling expansion. The results are shown in Figs. 1(b) and 2(b).

The calculated doubly differential cross sections are in reasonable agreement with experiment except for D^+ energies >8 eV. This is not surprising because this is the region where DI becomes important [Fig. 2(a)] and the corresponding channels are not included in the calculations. The agreement is also reasonable for the singly differential cross sections [Figs. 1(b) and 2(b)] except for very low electron energies. The analysis of the final state wave function allows us to separate the individual channels contributing to IE and AI. At D^+ energies of ~ 5 eV, ionization through the $^2\Pi_u(2p\pi_u)$ threshold is the dominant process; however, its sole contribution is not enough to explain all features observed experimentally. Indeed, higher channels are responsible for the second maximum observed in Fig. 2(b). The discrepancy with experiment around this second maximum indicates that IE leads to highly excited D_2^+ states not included in the theory (namely, beyond the 11th D_2^+ state). Therefore one has to be very careful in trying to fit the total D^+ distribution to an incoherent sum of FC factors associated with only a few IE channels. Although such a procedure may lead to DSI, IE, and DI distributions in qualitative agreement with experiment [26], it fails in predicting the correct contribution of each individual threshold.

The linear behavior observed between 1 and 4 eV in Fig. 1 is mainly due to autoionization of the Q_1 states and, to a lesser extent, of the Q_2 ones. The Q_3 and Q_4 states play a minor role. At very low D^+ energy (<1 eV) and electron energy ≤ 20 eV, the theory shows oscillations that are due to interferences between resonant and nonresonant ionization similar to those observed in dissociative photoionization [4]. Such oscillations are not seen in the present experiment due to the limited energy resolution, but they are responsible for the broadening of the linear structure at a D^+ energy of ~ 1 eV.

The previous comparison between theory and experiment and a more detailed analysis of the coincidence measurements allows us to extract fully differential cross sections for the different channels. As an illustration, Fig. 3 shows the electron angular distribution in the plane formed by the projectile beam and the D_2 molecules oriented perpendicularly to it. The two selected energy windows correspond to regions of the coincidence spectrum in which IE and AI dominate, respectively. In both cases, the angular distribution tries to follow the molecular axis because, at the high collision energy considered in this work, momentum transfer is more or less perpendicular to the incoming projectile direction. This is similar to what is observed in dissociative photoionization [21]. Nevertheless, the IE distribution is clearly asymmetric with respect to the molecular axis: more electrons are emitted in the forward (0°–90° in the D^+ side or 270°–360° in the D side) than in the backward (90°–180° in the D^+ side or 180°–270° in the D side) directions. Thus the asymmetry is the signature of the attractive interaction between the ejected electron and

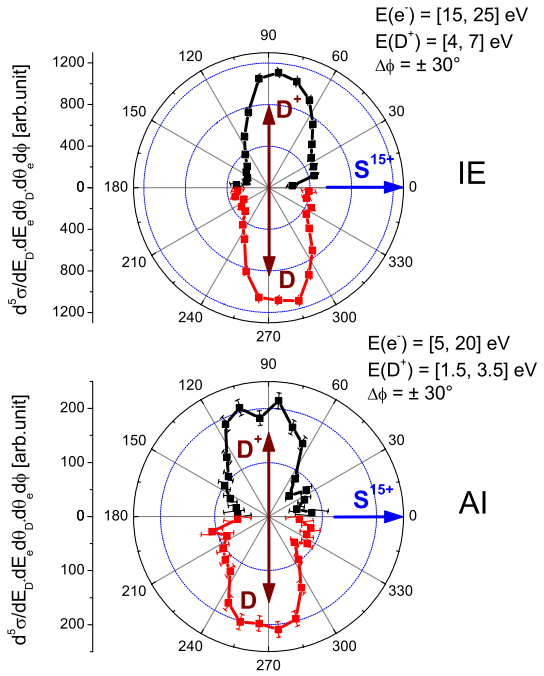

FIG. 3 (color online). Electron angular distribution in the plane formed by the projectile beam and the D_2 molecules oriented perpendicularly to it. The selected energy windows of ejected electrons and D^+ ions correspond to regions of the coincidence spectrum in which IE and AI dominate. $\Delta\phi$ indicates the azimuthal angular window.

the projectile. Although the projectile and the D^+ ion repel each other, no asymmetry has been observed in the D^+ angular distribution due to the large mass of D^+ compared to that of the electron. This is consistent with observing the same electron angular distribution on both the D^+ and D sides (see Fig. 3). In contrast, the AI distribution is nearly symmetric with respect to the molecular axis, except for the additional lobes observed at around 30° and 330°. The symmetry comes from the fact that autoionization is significantly delayed with respect to direct ionization, so that the projectile is very far away when the electron is ejected, and therefore, the effect of the projectile attractive interaction is less pronounced. The origin of the additional lobes at 30° and 330° is not so easy to understand, but it certainly must be related to the strong electron correlation in the doubly excited states that autoionize. Similar or even more complicated lobe structures have been found in photoionization experiments in the region of DESs [21]. It is worth noting here that the latter photoionization experiments (in the region of the Q_1 states) have revealed angular patterns that are slightly different along the D and D^+ directions. The limited statistics of the present experiment does not allow us to conclude if a similar effect also exists in collisions with fast ions.

In conclusion, we have performed kinematically complete experiments of dissociative ionization of D_2 by impact of fast ions. As in photoionization, autoionization from DESs play a crucial role. In contrast, unusually large contributions from ionization excitation and double ionization are observed in the electron-D^+ correlation spectra, in agreement with accurate theoretical calculations. The measured electron angular distributions from fixed-in-space molecules reveal (i) the signature of electron correlation in the autoionization process and (ii) a backward-forward asymmetry in the ionization excitation process that is due to the postcollisional projectile-electron interaction. These results show that kinematically complete collision experiments are ideal to investigate a large variety of ionization mechanisms, even larger than in photoionization experiments.

Calculations were carried out at the CCC-UAM. Work was supported by the DGI Project No. BFM2003-00194 (Spain), the European COST action D26/0002/02, the European HITRAP RTD Project No. HPRI-CT-2001-50036, and the France-Spain program PICASSO HF04-13.

[1] S. Strathdee and R. Browning, J. Phys. B **12**, 1789 (1979).
[2] C. J. Latimer, J. Geddes, M. A. MacDonald, N. Kouchi, and K. F. Dunn, J. Phys. B **29**, 6113 (1996).
[3] K. Ito, R. I. Hall, and M. Ukai, J. Chem. Phys. **104**, 8449 (1996).
[4] I. Sánchez and F. Martín, Phys. Rev. Lett. **79**, 1654 (1997).
[5] I. Borges, Jr. and C. E. Bielschowsky, J. Phys. B **33**, 1713 (2000).
[6] K. Ito, J. Adachi, R. Hall, S. Motoki, E. Shigemasa, K. Soejima, and A. Yagishita, J. Phys. B **33**, 527 (2000).
[7] W. Vanroose, F. Martín, T. N. Rescigno, and C. W. McCurdy, Science **310**, 1787 (2005).
[8] N. Lermer, B. R. Todd, N. M. Cann, Y. Zheng, C. E. Brion, Z. Yang, and E. R. Davidson, Phys. Rev. A **56**, 1393 (1997).
[9] N. Kouchi, M. Ukai, and Y. Hatano, J. Phys. B **30**, 2319 (1997).
[10] A. K. Edwards and Q. Zheng, J. Phys. B **34**, 1539 (2001).
[11] J.-Y. Chesnel, D. Martina, P. Sobocinski, O. Kamalou, F. Frémont, J. Fernández, and F. Martín, Phys. Rev. A **70**, 010701(R) (2004).
[12] A. K. Edwards, R. M. Wood, and M. F. Steuer, Phys. Rev. A **16**, 1385 (1977).
[13] R. M. Wood, A. K. Edwards, and M. F. Steuer, Phys. Rev. A **15**, 1433 (1977).
[14] B. G. Lindsay, F. B. Yousif, F. R. Simpson, and C. J. Latimer, J. Phys. B **20**, 2759 (1987).
[15] E. Y. Kamber, C. L. Cocke, S. Cheng, J. H. McGuire, and S. L. Varghese, J. Phys. B **21**, L455 (1988).
[16] E. Wells, I. Ben-Itzhak, K. D. Carnes, and V. Krishnamurthi, Phys. Rev. A **60**, 3734 (1999).
[17] I. Ben-Itzhak, E. Wells, D. Studanski, V. Krishnamurthi, K. D. Carnes, and H. Knudsen, J. Phys. B **34**, 1143 (2001).
[18] W. Wolff, I. Ben-Itzhak, H. E. Wolf, C. L. Cocke, M. A. Abdallah, and M. Stöckli, Phys. Rev. A **65**, 042710 (2002).
[19] R. Dörner *et al.*, Phys. Rev. Lett. **81**, 5776 (1998).
[20] Y. Hikosaka and J. H. D. Eland, Chem. Phys. **277**, 53 (2002).
[21] A. Lafosse, M. Lebech, J. C. Brenot, P. M. Guyon, L. Spielberger, O. Jagutzki, J. C. Houver, and D. Dowek, J. Phys. B **36**, 4683 (2003).
[22] T. Weber *et al.*, Phys. Rev. Lett. **92**, 163001 (2004).
[23] T. Weber *et al.*, Nature (London) **431**, 437 (2004).
[24] M. Takahashi, N. Watanabe, Y. Khajuria, Y. Udagawa, and J. H. D. Eland, Phys. Rev. Lett. **94**, 213202 (2005).
[25] C. Dimopoulou *et al.*, Phys. Rev. Lett. **93**, 123203 (2004).
[26] A. K. Edwards, R. M. Wood, J. L. Davis, and R. L. Ezell, Phys. Rev. A **42**, 1367 (1990).
[27] I. Ben-Itzhak, V. Krishnamurthi, K. D. Carnes, H. Aliabadi, H. Knudsen, U. Mikkelsen, and B. D. Esry, J. Phys. B **29**, L21 (1996).
[28] I. Sánchez and F. Martín, Phys. Rev. A **60**, 2200 (1999).
[29] F. Martín, J. Phys. B **32**, R197 (1999).
[30] I. Sánchez and F. Martín, J. Chem. Phys. **106**, 7720 (1997).
[31] I. Sánchez and F. Martín, J. Chem. Phys. **110**, 6702 (1999).
[32] J. Fernández and F. Martín, J. Phys. B **34**, 4141 (2001).